Use of TOPEX/Poseidon Sea Level Data for Ocean Analyses and ENSO Prediction: Some Early Results

MING JI, RICHARD W. REYNOLDS, AND DAVID W. BEHRINGER

National Centers for Environmental Prediction, NOAA, Washington, D.C.

(Manuscript received 2 February 1998, in final form 19 March 1999)

ABSTRACT

In this study, two sets of Pacific Ocean analyses for 1993–96 were analyzed. Both analyses were produced with the assimilation of subsurface temperature data from expendable bathythermographs and tropical atmosphere–ocean moorings. In addition one analysis also assimilated sea level data from TOPEX/Poseidon. Sea level variability in the two analyses agreed well with each other, and both agree with tide gauge and altimetry data for 1993–95. However, beginning in late 1995 through 1996, large sea level differences of 5–8 cm were found in the tropical western Pacific between the two analyses. Furthermore, large sea level discrepancies were also found between dynamic height estimated from TAO temperatures and tide gauge–altimetry observations in the same region during 1996. These discrepancies are consistent with the sea level differences between the two model based analyses.

Historical conductivity–temperature–depth data along 165°E near the equator were also analyzed and it was found that salinity variability on interannual timescale can result in a sea level variability of at least −5 dyn cm to +6 dyn cm. These results suggest that the sea level discrepancy in 1996 is likely due to inadequate salinity information both in estimating dynamic height from TAO temperature and in the data assimilation system used here, which corrects only temperature field.

The sea level error that resulted from inadequate salinity variability has a significant projection onto the second sea level anomaly EOF, which is linked to the onset phase of ENSO. This suggests that the error in the ocean initial conditions due to underestimate of interannual salinity variations in 1996 could impact the accuracy of ENSO prediction. Results from a twin experiment that uses two summer 1996 ocean initial conditions to hindcast for winter 1996/97 equatorial Pacific SST anomalies appear to support this hypothesis.

The results also pointed to a weakness of the present univariate assimilation system, which corrects only temperature. The improved sea level variability comes at the expense of reduced accuracy in temperature. A better solution would be a bivariate data assimilation system, which corrects both salinity and temperature, producing more accurate and consistent ocean initial conditions for ENSO prediction.

1. Introduction

During the Tropical Ocean Global Atmosphere (TOGA, 1985–94) decade, the ocean observing network for the tropical Pacific was vastly improved (McPhaden et al. 1998) to support both seasonal to interannual climate studies and prediction. The central element of the TOGA observing system for ENSO prediction is the tropical atmosphere–ocean (TAO) array of moored buoys (McPhaden 1993), which includes observations of subsurface temperatures in the equatorial Pacific. Additional subsurface temperature measurements over a broader geographic extent are provided by the low-density expendable bathythermographs (XBTs) network. However, despite the improved temporal and spatial coverage provided by TAO and the XBTs, subsurface oceanic observations are still considered spatially sparse and temporally sporadic, except at the limited number of TAO mooring sites. In particular, there are very few observations for subsurface salinity that also contribute to variations in the upper ocean density field. The launching of the TOPEX/Poseidon (T/P hereafter) satellite (Cheney et al. 1994) provided an unprecedented opportunity to observe sea level variability of the oceans with near-global coverage at about 10-day intervals. Although the satellite sea level dataset provides new opportunities to observe and study mid- and high-latitude oceanographic variability, it is our particular interest to explore the impact of T/P sea level data on the initialization of the tropical Pacific Ocean for ENSO predictions.

Carton et al. (1996) found that assimilation of T/P data can help to resolve major features of the seasonal cycle. Fischer et al. (1997) used sea level data derived from more than a decade of Pacific Ocean analyses produced by National Centers for Environmental Prediction

Corresponding author address: Dr. Ming Ji, Climate Modeling Branch, National Centers for Environmental Prediction, 5200 Auth Road, Rm. 807, Camp Springs, MD 20746.
E-mail: ming.ji@noaa.gov

(NCEP) to investigate the potential benefit of using sea level data for ENSO prediction. They compared skills from parallel prediction experiments, which were initialized by assimilation of sea level data and by assimilation of subsurface temperature data. Their results indicate that the ENSO prediction skill, obtained by the assimilation of sea level data, is comparable to that obtained by the assimilation of subsurface temperature data. Hence, they suggested that a positive impact on ENSO prediction skill can be expected when the assimilation of altimetric sea level data is used for ocean initialization. An ocean data assimilation system that is capable of assimilating sea level variability data as well as subsurface temperature data has been developed at NCEP (Behringer et al. 1998). TOPEX/Poseidon data have been available since October 1992. However, in late 1996, the National Oceanic and Atmospheric Administration (NOAA) Laboratory for Satellite Altimetry began to supply T/P data to NCEP in real time (Cheney et al. 1996). The real-time T/P data is used together with subsurface temperature data to experimentally produce Pacific Ocean analyses that are used as initial conditions for the NCEP coupled model for ENSO forecasts. In addition, Pacific Ocean analyses with assimilation of T/P data and subsurface temperature data have been retrospectively produced for 1993–96, and hindcast experiments are being carried out using ocean initial conditions produced both with and without assimilating the T/P data. In this paper, we will begin the examination of the impact of T/P altimetric sea level data on real-time and retrospective ENSO predictions.

The rest of this paper is organized as follows. Section 2 briefly describes the NCEP ocean data assimilation system and ocean analyses for 1993–96, which are produced with and without the assimilation of T/P data. In section 3, the 4-yr Pacific Ocean analyses are compared with tide gauge sea level data and real-time subsurface temperature data collected by the TAO moorings. We further compare tide gauges, altimetry, and TAO-dynamic heights in section 4 to examine the origin of two differing sea level trends found between the two model analyses. We then discuss in section 5 reasons for the differing sea level trends found both from validation of the models and from the comparison of observational data. In section 6, we present results from coupled model predictions using ocean initial conditions produced with and without assimilating T/P data. We summarize our results in section 7 and discuss how to best utilize sea level data for producing the best possible ocean analyses for ENSO prediction.

2. The analysis system

The NCEP's ocean analysis system includes an ocean general circulation model configured for the Pacific and an ocean model–based three-dimensional variational data assimilation system, which is extended from a system developed by Derber and Rosati (1989). The ocean model was developed at the Geophysical Fluid Dynamics Laboratory and is known as Modular Ocean Model (Bryan 1969; Cox 1984; Philander et al. 1987). Presently, the model domain covers the Pacific from 45°S to 55°N and 120°E to 70°W with 28 vertical levels. The model has a zonal resolution of 1.5° and meridional resolution of one-third° in the tropical Pacific within 10° of the equator. The meridional resolution gradually reduces to 1° poleward of 20° latitude. Our main extension to the Derber and Rosati (1989) scheme is the incorporation of a vertical error variance function for the first guess, which also provides a mechanism to allow assimilation of sea level observations. Details of the ocean analysis system can be found in Ji et al. (1995) and Behringer et al. (1998).

The incorporation of the vertical error covariance function in our extended ocean data assimilation scheme provides a simple avenue to allow assimilation of sea level data, which is introduced as an additional constraint. The variational data assimilation scheme minimizes a functional,

$$\mathbf{I} = \mathbf{T}^{\mathrm{T}}\mathbf{E}^{-1}\mathbf{T} + [D(\mathbf{T}) - \mathbf{T}_0]^{\mathrm{T}}\mathbf{F}^{-1}[D(\mathbf{T}) - \mathbf{T}_0] + [D(L\mathbf{T}) - \delta\mathbf{Z}_0]^{\mathrm{T}}\mathbf{G}^{-1}[D(L\mathbf{T}) - \delta\mathbf{Z}_0], \quad (1)$$

where $\mathbf{T}$ represents the correction to the first-guess temperature field computed by the model, $\mathbf{E}$ is the first-guess error covariance matrix, $\mathbf{T}_0$ represents the difference between the temperature observations and the first-guess field, D is an interpolation operator that transforms the first-guess field from the model grid to the observation locations, $\mathbf{F}$ is the observation error covariance matrix for temperature, L is a linear operator that transforms a vertical column of temperature corrections into an estimate of the correction to the first-guess sea surface height field, $\mathbf{G}$ is the observation error covariance matrix for sea surface height, and $\delta\mathbf{Z}_0$ represents the difference between the observed and first-guess sea surface height fields. Currently, the observational errors are assumed to be uncorrelated, so the matrices, $\mathbf{F}$ and $\mathbf{G}$, have only diagonal elements, which are the error variances for the data.

The first two terms on the right-hand side of (1) are for the assimilation of surface and subsurface temperature observations. The third term on the right-hand side of (1) is a constraint imposed by observations of sea surface height. The version of the ocean model that we use imposes a rigid lid at the surface so that the variable that is equivalent to sea surface height is the diagnosed surface pressure under the lid. It would be pointless to correct the diagnosed pressure itself (Pinardi et al. 1995); instead, the third term uses sea surface height observations to impose an integral vertical constraint on the corrected model temperature field. The relative sizes of these temperature corrections throughout the water column depends on the vertical structure of the first-guess error covariance. In other words, the assimilation system preferentially corrects the model temperature

field where the probability of its being in error is the greatest, making those corrections in such a way as to bring the model surface dynamic height into closer agreement with the sea surface height observations.

There are two implied assumptions. The first is that we can use the sea surface height observations to correct only the baroclinic part of the sea surface height and that it is safe to neglect the barotropic part. In the Tropics, which is our main region of interest, this may be a reasonable assumption (Chao and Fu 1995; Picaut et al. 1995). The second assumption is that to correct the surface-dynamic height we need only correct the temperature and corrections to salinity may be neglected. It is this second assumption that is being examined in the present study. Further details of the assimilation system and the choice of vertical error covariance for the first guess are described in Behringer et al. (1998).

For the present research, two sets of monthly mean ocean analyses for January 1993 to December 1996 are produced from the ocean analysis system. These analyses are produced by forcing the ocean model with monthly mean NCEP operational atmospheric analyses of near-surface winds, which are converted to stress using a constant drag coefficient, $C_d = 1.3 \times 10^{-3}$, and climatological heat fluxes from Oberhuber (1988). The ocean initial condition used for these analyses is the ocean state for 1 January 1992 obtained from a set of previously produced Pacific analyses. We ran the ocean model with assimilation of subsurface temperature data for January–December 1992 forced with the NCEP operational near-surface wind analyses for spinup. This is because the previous retrospective Pacific analysis was produced with a different wind stress forcing product. Two sets of monthly mean Pacific analyses are produced starting from 1 January 1993. Both sets assimilated subsurface temperature data from XBT and TAO moorings. However, one set of analyses also assimilated sea level data from T/P. We denote the analyses with assimilation of T/P data as NCEP–TP, and the analyses without using T/P data as NCEP–XBT.

A satellite altimeter does not directly measure the surface dynamic topography. In order to recover the dynamic topography from the T/P data, we would have to remove the topography of the geoid. Because the geoid is not accurately known, we assimilate only the variable part of the measured sea level. In our case, we define the sea level variability as the deviation from a 3-yr base period mean of January 1993–December 1995. This reference period is chosen because at the time the T/P assimilation system was developed (1996), T/P data had been complete for these three years. The assimilation of T/P data also requires an estimate of the model sea level deviation relative to the same base period mean. To achieve this, we first produced the NCEP–XBT analyses. The 1993–95 mean sea surface height from this set of analyses was determined and used as the model base period mean for T/P assimilation in NCEP–TP analyses. Note that the TAO moorings and most of XBTs in the tropical Pacific measure the thermal structure in only the upper 500–700 m of the ocean where most of the seasonal to interannual variability occurs. For this reason, our data assimilation system is configured to assimilate temperature data for the upper ocean between the surface and 720 m. For consistency, we only allow T/P data to have an influence within this depth range.

3. Validation of analyses

In this section, we compare the two sets of 4-yr Pacific analyses with in situ observations of sea level variability from the tide gauge network (Wyrtki 1979) and subsurface temperature observations from the TAO moorings. Note that the tide gauge data are not used for assimilation and therefore can be considered as independent verification. However, subsurface temperatures from the TAO moorings are used for assimilation and therefore are not independent. Nevertheless, by comparing temperature differences between the analyses and the TAO moorings, we can examine the change in the fit of the analyses to the TAO data due to the addition of T/P data.

The differences in sea level and the depth of 20°C isotherm along the equator between the two sets of analyses are shown in the left and right panels of Fig. 1, respectively, for the 4-yr period of 1993–96. A significant feature shown in this figure is that the sea level difference (left) between the two sets of analyses are within about 2–3 cm for nearly three years, that is, from 1993 to late 1995. This is within the range of observational error of the T/P data (Behringer 1994; Busalacchi et al. 1994). However, beginning in late 1995 throughout 1996, a significant difference between analyses with and without T/P data is seen in the western equatorial Pacific. The magnitude of the difference is as large as 8–10 cm during the summer of 1996. To a lesser degree, a similar feature is also found in the thermocline depth (depth of 20°C) differences (right). During 1996, the thermocline depth difference tends to be systematically positive in the western equatorial Pacific near the data line indicating that the NCEP–XBT analysis is deeper in this region than the NCEP–TP analysis. (There is also a smaller but opposite tendency in the thermocline difference in the eastern equatorial Pacific.)

The spatial characteristics of the sea level differences between analyses made with and without T/P data are shown in Fig. 2. Based on the results in Fig. 1, we divided the 4-yr period into two parts: 1993–95 and 1996. The average sea level differences for these two periods are shown in the upper and lower panels, respectively. Note that the contour interval for 1996 mean difference field is four times the interval for 1993–95 mean. Figure 2 illustrates that, for the first three years, analyses produced with or without T/P data are similar and well within the range of observational error. However, for 1996, there is a significant difference, espe-

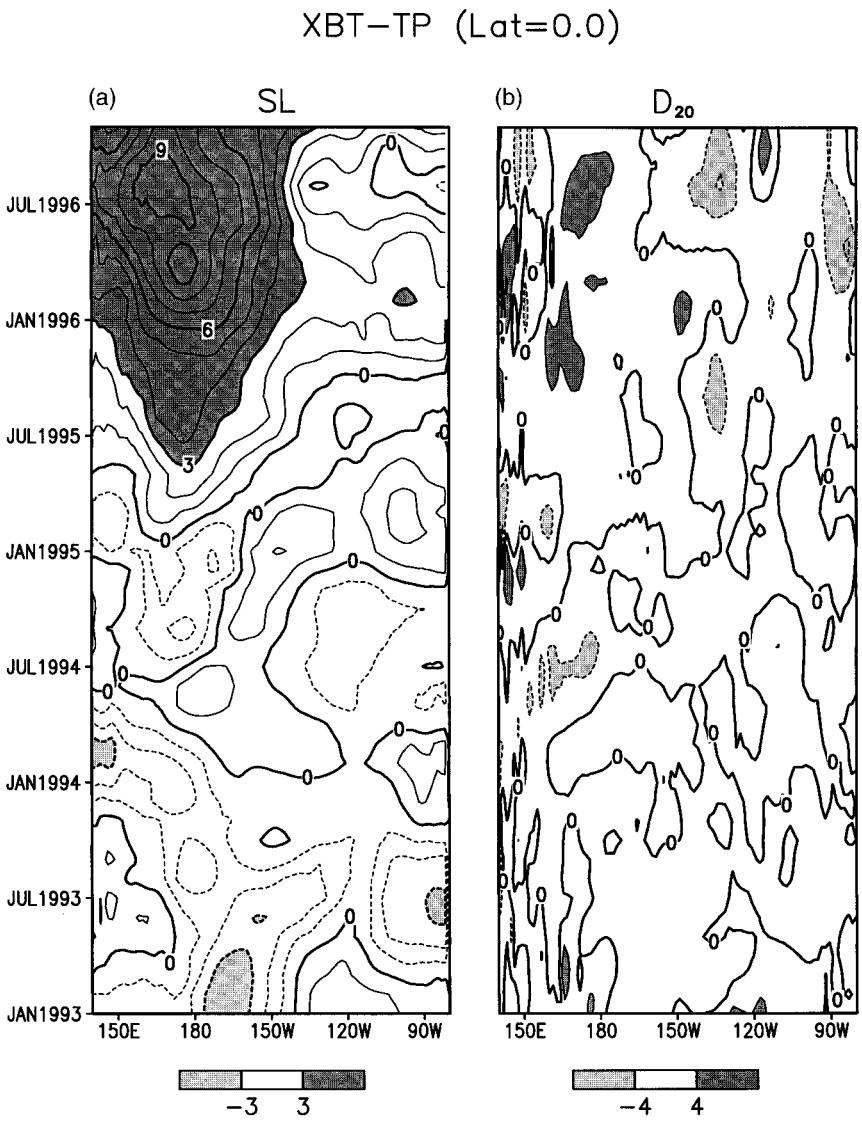

FIG. 1. (a) Sea level and (b) depth of 20°C isotherm (b) differences along the equator between NCEP–TP and NCEP–XBT for 1993–96. The contour interval for the sea level (depth of 20°C isotherm) differeces is 1 cm (4 m).

cially in the tropical Pacific within 10° of the equator. The largest difference occurs in the western Pacific centered near 5°S, 155°E.

The differences in sea level in the western Pacific between the two analyses found in 1996 are significant. The systematic difference in the thermocline slope along the equator could impact ENSO prediction results should these two analyses be used for initialization of coupled prediction models (see section 6). Therefore, it is important to identify the source of these differences and improve the assimilation system to produce consistent and realistic analyses. First, we need to determine whether there is error in our analysis system by validating these analyses directly against in situ observations. For this purpose, we compare the two analyses with the independent sea level observations from tide gauges and dependent subsurface temperature observations from the TAO moorings. Because the largest differences between the two sets of analyses are found in the western Pacific near the equator, we choose four tide gauge stations in this region. These are Kapingamarangi (1.1°N, 155°E), Nauru (0.5°S, 167°E), Tarawa (1.4°N, 173°E), and Kanton (2.8°S, 172°W). The tide gauge data at each station are processed to remove the 1993–1995 mean. Comparisons of sea level deviations for the two analyses and for tide gauge observations at these four locations are shown in Fig. 3. These results show that during the 1993–95 period the variability of both analyses agree with tide gauge data. However, starting in late 1995, the NCEP–TP analyses tend to follow

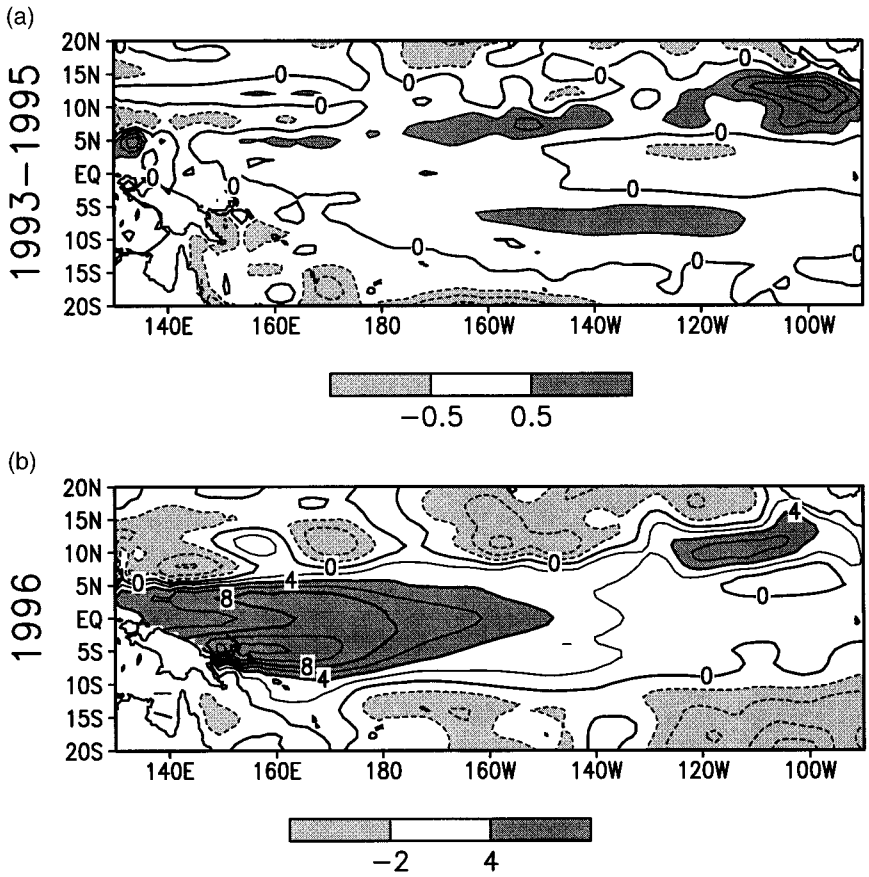

FIG. 2. (a) Average sea level differences between NCEP–TP and NCEP–XBT for 1993–95. Areas where the differences are below −0.5 cm (above 0.5 cm) are shaded in light (dark) shadings. Contour intervals are 0.5 cm. (b) Average sea level differences between NCEP–TP and NCEP–XBT for 1996. Areas where the differences are below −2 cm (above 2 cm) are shaded in light (dark) shadings. Contour intervals are 2 cm.

the tide gauge data while the NCEP–XBT analyses exhibit a trend of rising sea level, which deviates from both the NCEP–TP analyses and tide gauge data. The T/P and tide gauges are measuring the same variable and, therefore, it is not surprising that the NCEP–TP analyses agree better with the tide gauge data. However, these intercomparisons seem to suggest that the NCEP–XBT analyses of sea level are in error in the equatorial western Pacific in 1996. The differences in sea level variability are roughly 5–8 cm, which is significant for this region. It exceeds the observational error for both T/P and tide gauges, and it is close to the magnitude of sea level variability of 10–15 cm, which is associated with ENSO in the western equatorial Pacific.

Next, we validate the analyses by comparing them with in situ temperature observations. The best available in situ observations that have almost-continuous records for our region and time of interest are the subsurface temperature profiles from the TAO moored buoys. All of the available real-time TAO mooring data are assimilated in both analyses. Because the data assimilation produces a weighted combination of all data and the analysis first guess, residual discrepancies between analyses and observations will remain. Thus, comparison of the two analyses to the dependent TAO data can provide estimates of how well each analysis fits these observations. These comparisons were done at all TAO mooring sites between 5°S and 5°N in the western Pacific that had a reasonably continuous record during the 1993–96 period. The TAO data are averaged into a monthly mean for each mooring site at all available depths to compare with the monthly mean analyses. The root-mean-square (rms) differences between the analyses and selected western Pacific mooring sites are listed in Table 1. In addition, an example of differences between the analyses and the TAO mooring temperature is shown in Fig. 4.

From Table 1, we found that at most mooring sites both analyses have comparable rms differences relative to the mooring temperatures for 1993–95. However, for 1996, the rms temperature differences for the NCEP–TP analyses are generally larger than those for the NCEP–XBT analyses. Thus, in these areas during 1996 the NCEP–XBT analyses agree better with the TAO in

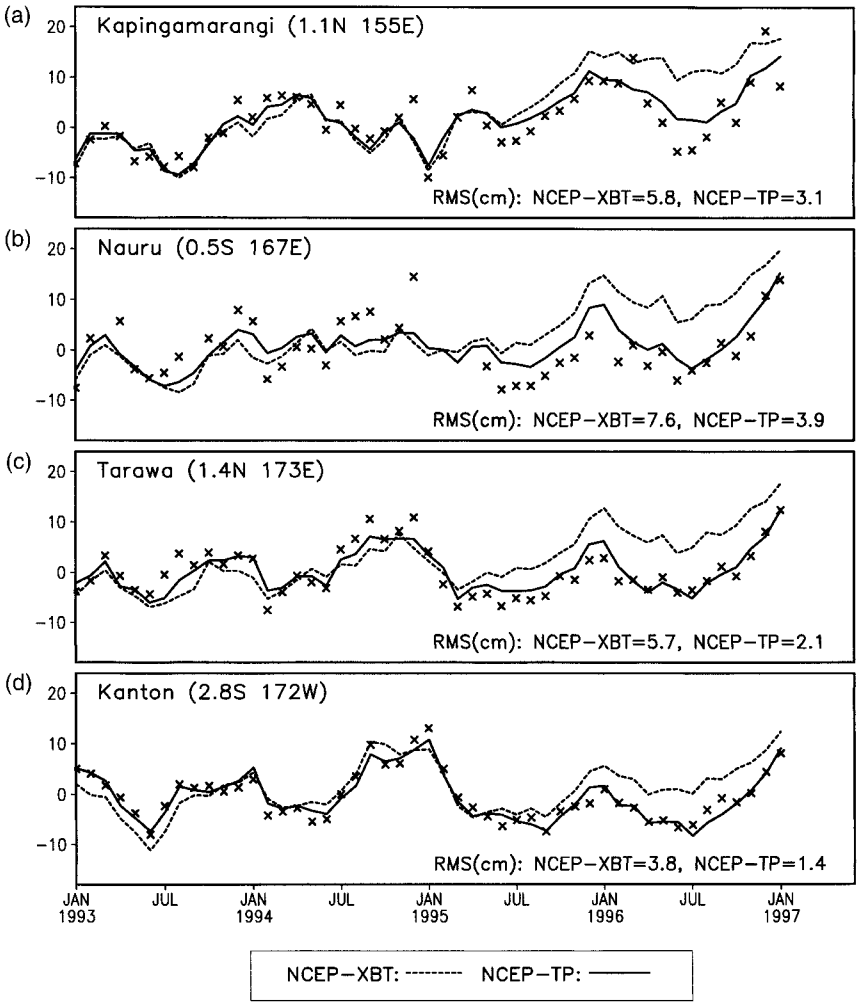

FIG. 3. Sea level variations at four tide gauge stations for NCEP–XBT (dashed), NCEP–TP (solid), and tide gauge data (shown in "×"s). Locations of the tide gauge stations and rms differences between analyses and tide gauge observations are shown in the figure.

TABLE 1. Rms differences (°C) between analyses and the monthly mean TAO mooring temperatures. The rms difference at each site is estimated over a two-dimensional domain (time, depth).

			1993–95		1996	
ID	Lat	Long	NCEP–XBT	NCEP–TP	NCEP–XBT	NCEP–TP
52309	5°N	180°	0.29	0.32	0.48	0.45
52003		165°E	0.32	0.36	0.34	0.44
52008		156°E	0.39	0.50	0.25	0.32
52302		147°E	0.45	0.44	0.35	0.41
51023	0°	155°W	0.39	0.37	0.26	0.39
51010		170°W	0.40	0.38	0.32	0.49
52311		180°	0.45	0.48	0.43	0.72
51019	5°S	155°W	0.30	0.37	0.29	0.47
51034		170°W	0.38	0.43	0.37	0.47
52313		180°	0.42	0.43	0.59	0.49
52010		156°E	0.57	0.56	0.56	0.72

situ observations of temperature than for NCEP–TP. We select one of the mooring sites listed in Table 1, at (0°, 180°), to illustrate the model–data difference in subsurface temperature (Fig. 4). [Note that this site is located between Tarawa (1.4°N, 173°E) and Kanton (2.8°S, 172°W), where for 1996 the sea levels from NCEP–TP analyses agree better with the tide gauge observations and are lower than the NCEP–XBT analyses; see Fig. 3.] The addition of T/P data results in general cooling of the upper ocean during 1996 at (0°, 180°) for NCEP–TP, which is required to reduce the sea level height. This leads to an increase in negative (cold) temperature errors below about 150-m depth, and also to a reduction of positive (warm) temperature errors in the vicinity of the thermocline.

4. Comparison of direct and indirect observations

Results from the model validation against in situ sea level and temperature observations suggest that there

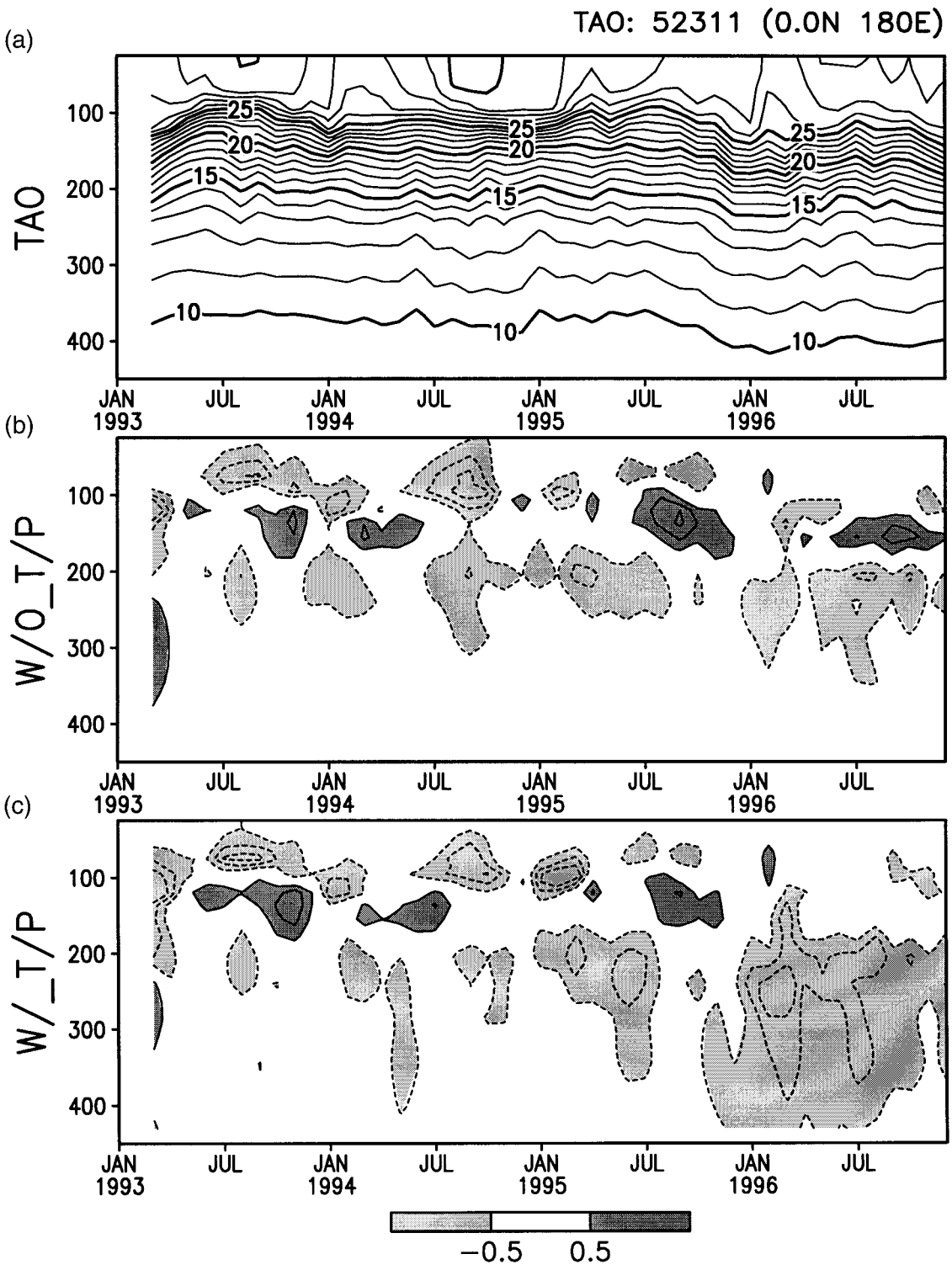

FIG. 4. Temperature differences (errors) between analyses and mooring observations for (b) NCEP–XBT and (c) NCEP–TP at (0°, 180°); (a) mooring temperatures. The contour interval for the difference fields is 0.5°C; the contour interval for the mooring temperatures is 1°C. For the difference fields, areas where temperature errors are greater (less) than 0.5°C (−0.5°C) are shaded light (dark). See Table 1 for rms differences between analyses and the mooring for 1993–95 and for 1996.

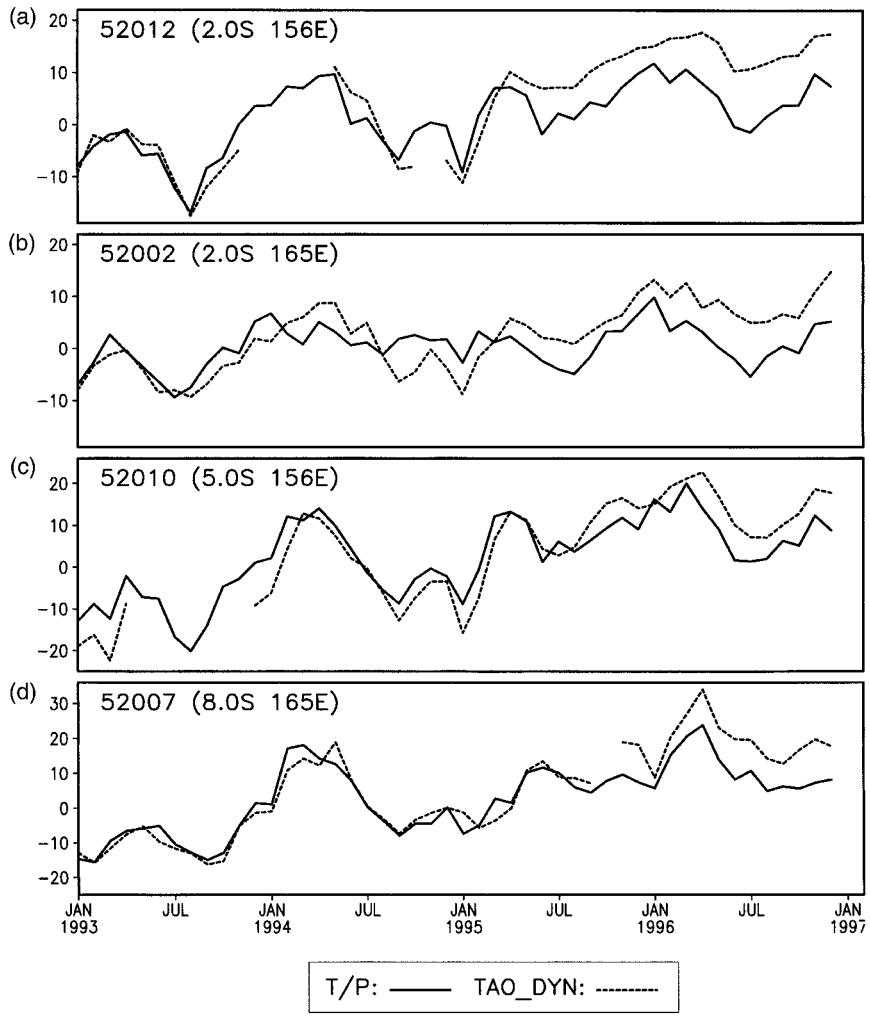

FIG. 5. Sea level-/dynamic-height variations at equatorial mooring sites: (solid) sea level deviations from T/P data at mooring sites; (dashed) dynamic height variations estimated from observed TAO mooring temperatures. All dynamic height and sea level variations are deviations from their respective 1993–95 mean. The dynamic height from moorings at each mooring site are estimated from surface to 500-m depth.

may be a discrepancy between the sea level and temperature observations for 1996 because changes in temperature alone cannot account for the changes in sea level. To investigate this possibility, we compare dynamic height variations estimated from the TAO mooring temperatures against T/P sea level variations and tide gauge observations. The dynamic heights relative to 500 m at each mooring site were obtained from NOAA's Pacific Marine Environment Laboratory (PMEL). The dynamic heights are estimated using subsurface temperature data from the TAO moorings and salinities obtained from the TAO temperatures using climatological temperature–salinity (T–S) relationships obtained from Levitus et al. (1994); see Kessler and Taft (1987) for details. The dynamic height variations from mooring data at several western Pacific sites along 165° and 156°E relative to their 1993–95 mean are shown in Fig. 5. The figure also shows the sea level deviations relative to the same base period from T/P data at these locations. These results show that the dynamic height from the moorings and the sea levels from T/P start to diverge in 1995 at all mooring sites. There is evidence for a trend in sea level in the TAO-dynamic heights starting in 1995 that is not present in the T/P data. The differences are similar to those found in the sea level comparisons between the NCEP–TP and the NCEP–XBT analyses and the tide gauges. These results indicate that sea level variability measured by T/P and sea level variability estimated from dynamic heights based on observed temperature and climatological T–S relationship may be inconsistent. The discrepancies are between roughly 5 and 10 cm at the sites in Fig. 5 during 1996.

A remaining question is whether this result is robust given that a partial reference period (1993–95) is cho-

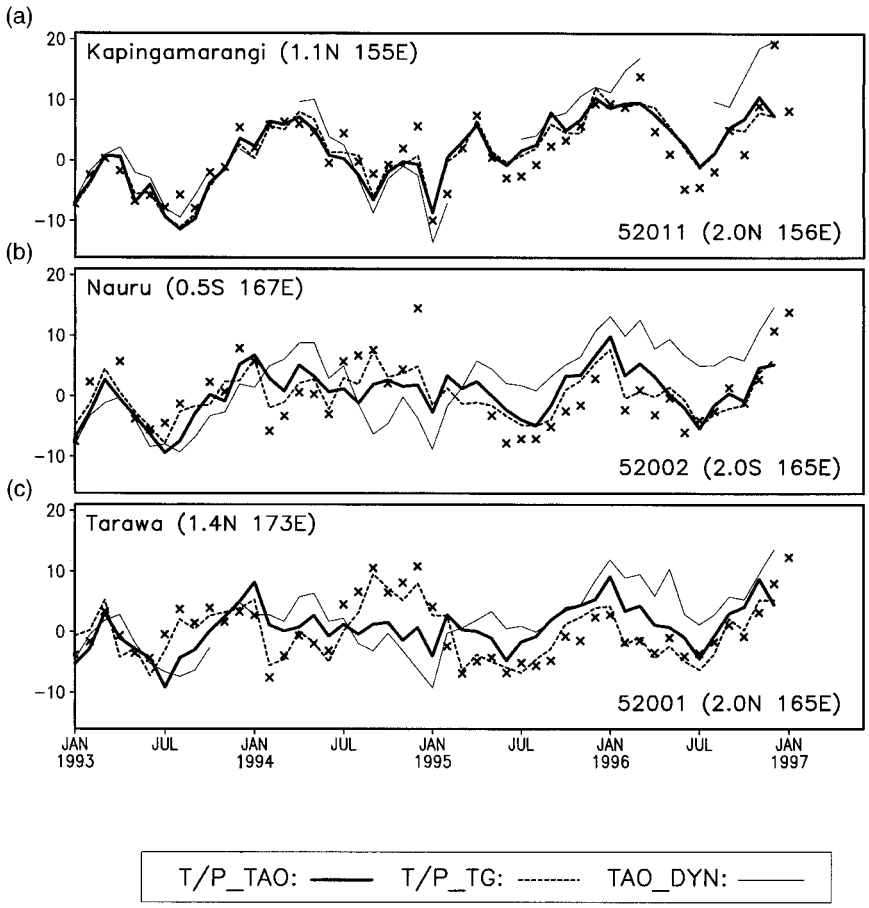

FIG. 6. Sea level-/dynamic-height variations at four tide gauge stations in the western equatorial Pacific. The mooring sites are chosen to be the nearest to these tide gauge stations. Sea level variations from T/P at mooring sites (heavy solid); dynamic height variations estimated from TAO mooring temperatures (thin solid); sea level from T/P at tide gauge stations (dashed); tide gauge data ("×"s). Locations of tide gauge and moorings are indicated in the figure.

sen. We should point out that the important message from comparisons shown in Fig. 5 is that the two datasets, TAO-dynamic height and T/P, are actually showing different trends during the 1993–96 period. A significant sea level trend that suggests a 5–10-cm sea level rise from 1993 to 1996 in the western equatorial Pacific is seen in TAO-dynamic height but is essentially missing in T/P. This difference in sea level trends is independent of the choice of reference period.

We have also compared T/P-and TAO-derived sea level variability with in situ observations of sea level variability from tide gauges. There were three tide gauge stations within 5°S and 5°N in the western equatorial Pacific west of the date line. These are Kapingamarangi (1.1°N, 155°E), Nauru (0.5°S, 167°E), and Tarawa (1.4°N, 173°E). Data from a fourth tide gauge station at Rabaul (4.2°S, 152°E) were also available. However, a subsidence of 1–2 cm yr^{-1} has been found, possibly due to volcanic activities in the region (R. Cheney 1997, personal communication). Therefore, this station was not used for comparison. Shown in Fig. 6 are the sea level variability at the above three tide gauge stations and the dynamic height variability at three nearest TAO mooring sites as identified in the figure. We also show in this figure the sea level variability of T/P data at both the three mooring sites and at the three tide gauge locations. This was done to account for the spatial variability in the sea level signal between the moorings and island locations. Note that the nearest mooring to Nauru (0.5°S, 167°E) was at (0°, 165°E). However, the 1996 data at this site were not available, so we used the (2°S, 165°E) mooring instead. The results are similar to those shown in Fig. 5, and where differences are small, the T/P data and the tide gauges tend to agree better with each other than they agree with the dynamic heights. These results suggest that the sea level variability estimated from the TAO dynamic height for 1996 may be in error in the equatorial western Pacific region.

5. Discussion

The comparisons shown in sections 3 and 4 suggest that there is a significant difference in sea level trends

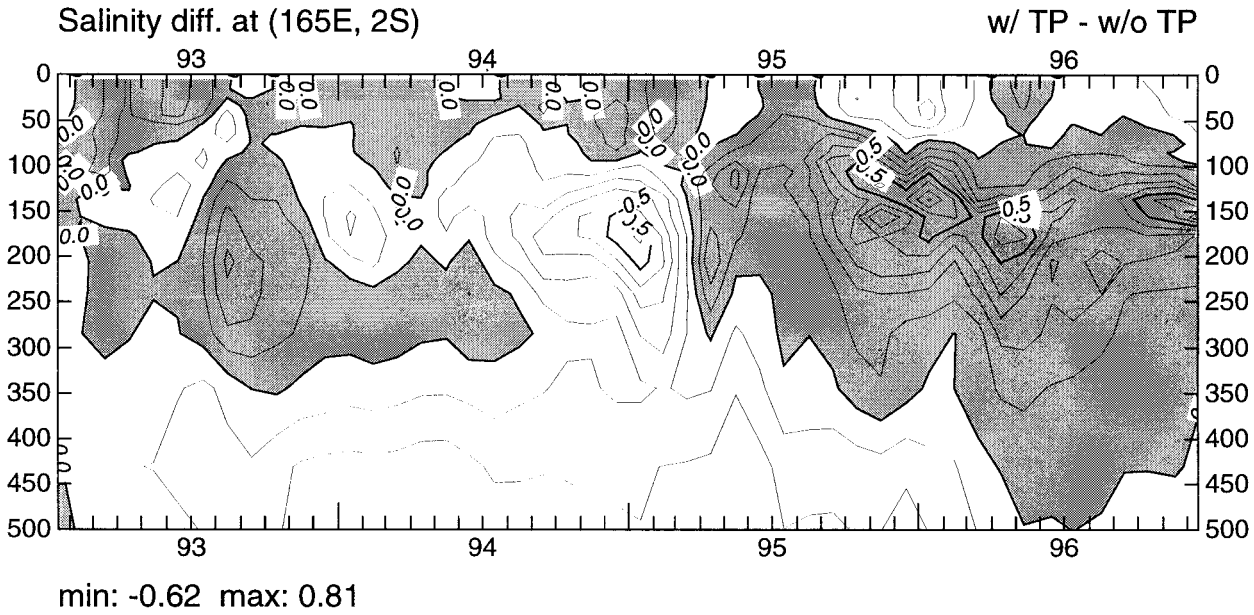

FIG. 7. Salinity difference (NCEP–TP minus NCEP–XBT) at (2°S, 165°E) for 1993–96. The contour interval is 0.1 psu. Areas of positive difference are shaded.

between sea level estimated from the TAO temperatures and from T/P and tide gauge observations for 1995–96. If we can assume that it is safe to neglect the barotropic part of the sea surface height change, then the most likely explanation for such discrepancy in sea level is the lack of salinity information. Our data assimilation scheme assumes that model–data differences in both temperature and sea level are due to errors in model temperatures alone. However, this assumption may not be always valid. Sea level variability is caused by variations in both temperature and salinity, especially in the western tropical Pacific. Emery and Dewar (1982) estimated a dynamic height error of 4 cm if salinity was not included; Kessler and Taft (1987) found large salinity effects in the central Pacific during the 1982–83 El Niño; McPhaden et al. (1990) found a 4-cm sea level error in the western Pacific during 1986–87 El Niño when mean *T–S* was used to compute dynamic height instead of using observed salinity data. Recently, Maes (1998) and Kessler (1999) both have found evidence that over broad regions of the tropical ocean, there are large interannual salinity variations and their effects on sea level are sufficiently large that they could be detected by an altimeter. These studies indicated the importance of the contribution of salinity to sea level variations. However, because our model does not have realistic freshwater flux forcing, it does not reproduce realistic salinity variations. Also, because the TAO dynamic heights were computed using salinity from a mean *T–S* relationship, they lack the full effect of the actual unobserved salinity, which may largely account for the differences between the dynamic height and the T/P sea level during 1996.

In this section, we will provide evidence to support our hypothesis that the differing sea level trends found both in model–model comparisons and in direct–indirect observation comparisons are due to an underestimate of salinity. This is done by examining the effects of data assimilation on model temperature and salinity fields and by examining the historical subsurface salinity observations to search for evidence of large interannual salinity signals.

Our present data assimilation system is a univariate scheme that corrects only the temperature field to minimize the model–data misfit. Errors in the variability of model salinity, which also affect sea level, are not directly corrected by the assimilation system. The addition of T/P data resulted in a different model–temperature data fit that satisfied the additional constraint in sea level but at the expense of a larger residual difference between model temperature and observed temperatures from TAO moorings and XBTs. However, the different model–temperature data fit due to the addition of T/P data results indirectly in changes in the model salinity field. Shown in Fig. 7 is the salinity difference at (2°S, 165°E) between the two analyses (NCEP–TP minus NCEP–XBT) during the entire 4-yr period. Positive salinity differences during the late 1995 to 1996 period indicates that the NCEP–TP analysis has a higher salinity at this location during that time. Analyses of the velocity fields from both datasets (not shown) indicate that the differences in salinity are due to differences in the three-dimensional advection fields. Note that the salinity increase during the 1995–96 period for NCEP–TP leads to a lower model sea level. This suggests that in this case the assimilation of altimetry data also had a positive

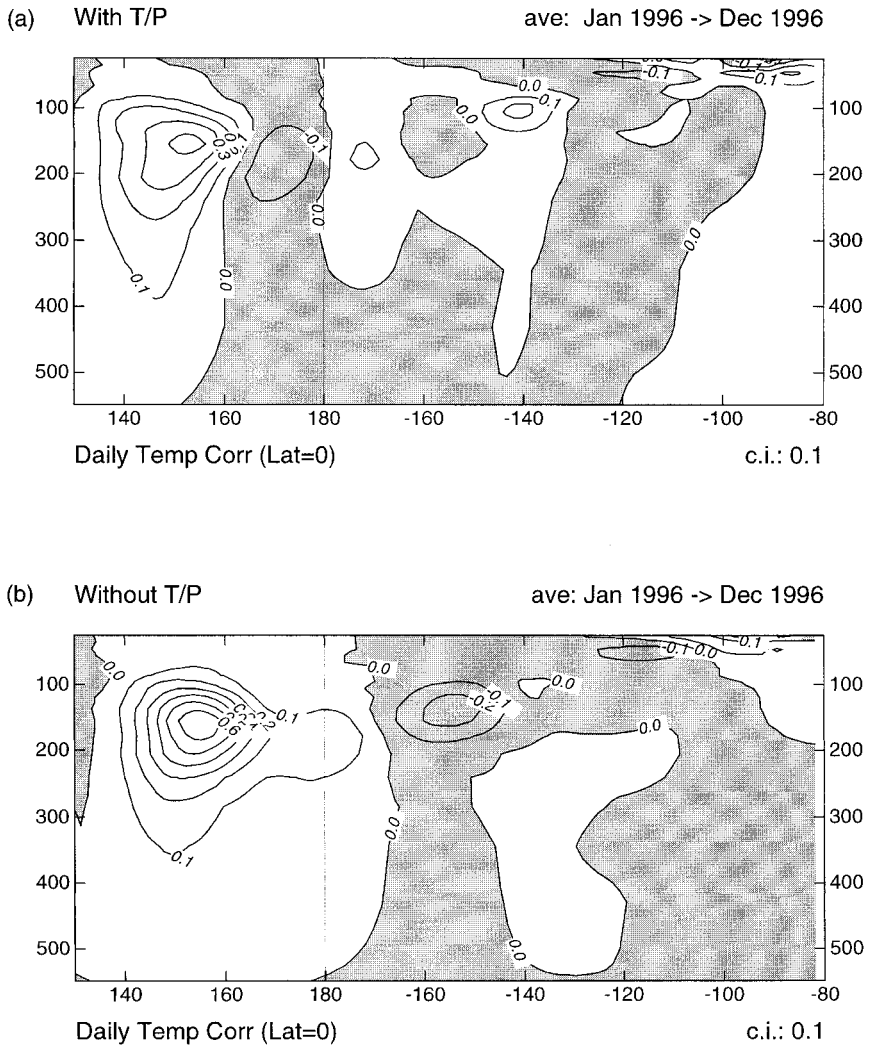

FIG. 8. Average daily temperature correction for 1996 along the equator. (a) NCEP–TP (b) NCEP–XBT. The contour interval is 0.1°C day^{-1}. Areas of negative temperature corrections (cooling) are shaded.

impact on the model salinity field, changing it in the correct sense to reduce sea level error. However, to get a truly correct salinity variability in the model will require that the model has both an accurate advection field and an accurate salinity source. These are not achieved by the model due to errors in both model and the forcing field. The remaining sea level error due to insufficient salinity variability has to be compensated by relaxed temperature data fit.

This is demonstrated by examination of the average temperature correction along the equator for 1996 (Fig. 8). These are the changes added to the model temperature field by data assimilation. Without T/P data, the data assimilation scheme attempts to minimize only the temperature data misfit. The result is large positive temperature correction (warming) throughout the water column in the western Pacific west of the date line (lower panel). When T/P data are added, the assimilation scheme must satisfy an additional constraint from the T/P data to achieve lower sea level in the western Pacific. Because our present assimilation system is univariate, the only way to accomplish this is through a relative cooling of the ocean in this region. The result is reduced positive temperature correction in the western Pacific west of the date line (upper panel). Thus, the reduction of the temperature correction to near 0.2°C day^{-1} in the NCEP–TP analysis for 1996 results in a higher temperature analysis error but in a much reduced sea level error.

These analyses suggest that inaccurate salinity could be a plausible reason for the differences between NCEP–XBT and NCEP–TP analyses and the inconsistency between dynamic heights and T/P sea level during 1996. To estimate the size of salinity signal that can lead to 5 cm of sea level error, we computed the dynamic height near the equator at 165°E using TAO temperatures and

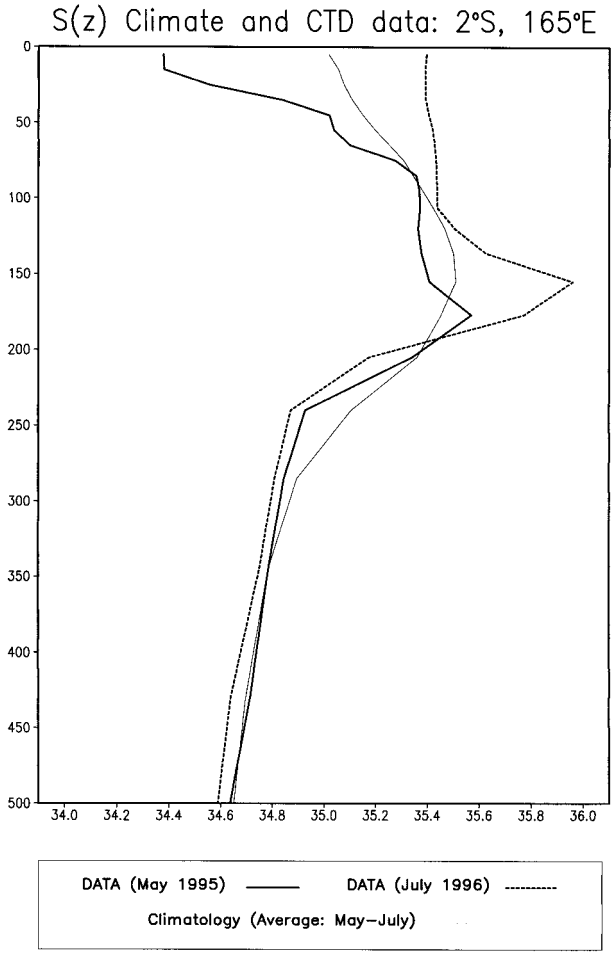

FIG. 9. Salinity profiles at (2°S, 165°E) for May 1995 (heavy), July 1996 (dashed), and the Levitus et al. (1994) climatology (light). The climatology is the average of May and Jul at this location.

the Levitus et al. (1994) salinity climatology. We then found that an average perturbation in salinity of 0.5 psu throughout the upper 130 m would result in a sea level change of 5 dyn cm (not shown).

To determine whether a perturbation of this size is realistic, we obtained conductivity–temperature–depth (CTD) data from NOAA/PMEL (Ando and McPhaden 1997) and examined the observed salinity profiles at (2°S, 165°E). Although these data are sparse, two salinity profiles at this location taken in May 1995 and July 1996 were available and are shown in Fig. 9. An average of the May and July climatological salinity profiles at this location (Levitus et al. 1994) is also shown in the figure for reference. Note that the May and July climatological salinity profiles at this location differ from each other by roughly 0.2 psu in the top 60 m and much less below 100 m. The figure shows two depth ranges where the differences between the 1996 and 1995 profiles exceeds 0.5 psu: from the surface down to roughly 40 m and in the thermocline around 150 m. The salinity perturbation (deviation from the Levitus climatology) based on the July 1996 profile was sufficient to generate a dynamic height signal exceeding 5 dyn cm. Furthermore, because the salinity increased from 1995 to 1996, the sign as well as the magnitude of the change is consistent with the difference between the dynamic height and sea level observations in Figs. 5 and 6.

The number of CTD profiles for the period of 1995–96 is very limited. In general, the observed subsurface salinity data are too few to construct a three-dimensional salinity field. Therefore, it is not certain that the salinity signal found in the profile shown in Fig. 9 is representative for 1996. However, CTD profiles are more abundant during earlier periods in the western tropical Pacific, particularly along 165°E (Ando and McPhaden 1997). To further the argument that an underestimate of the salinity variability is a likely cause of the inconsistency between the TAO dynamic height and T/P sea level, we computed, for the period 1979–96, two estimates of the dynamic height (relative to 500 m) along 165°E, first, using observed $T(z)$ and $S(z)$ profiles and, second, using the observed $T(z)$ profiles and $S(z)$ based on the observed $T(z)$ and the climatological mean T–S (Levitus et al. 1994). The dynamic height differences were computed on a monthly 1° latitude grid for all profiles between 162° and 168°E where the sign of the difference is dynamic height using T–S relationship minus the dynamic height based entirely on observations. The differences are shown in Fig. 10 for the period January 1984 to July 1989. This period was selected so that there were at least two months of CTD observations per year. Even with this restriction, 81% of the gridded array had to be filled by interpolation. A Cressman (1959) method was chosen for the interpolation to avoid producing interpolated values that are local maxima. With these limitations, Fig. 10 shows several regions with differences above 5 dyn cm and below -5 dyn cm. At 2°S, the range is -5 to 6 dyn cm. This range, which is due to the missing interannual salinity variability, is approximately the same size as the discrepancies between the two model-based analyses and is additional circumstantial evidence that the difference between the analyses could be due to salinity.

6. Implications for ENSO prediction

At NCEP, our main uses for routine analyses of the Pacific Ocean are to monitor the development of ENSO and to initialize a coupled prediction model for forecasting the equatorial Pacific SST variability associated with ENSO. Our past experience shows that one of the key factors that contributes to our ENSO prediction skill is the initialization of the ocean by assimilating observed surface and subsurface temperature data (Ji and Leetmaa 1997). In the previous section we showed that when T/P data were assimilated as well, the result was a significant change in sea level in the analyses for 1996. These changes in sea level reflect corresponding chang-

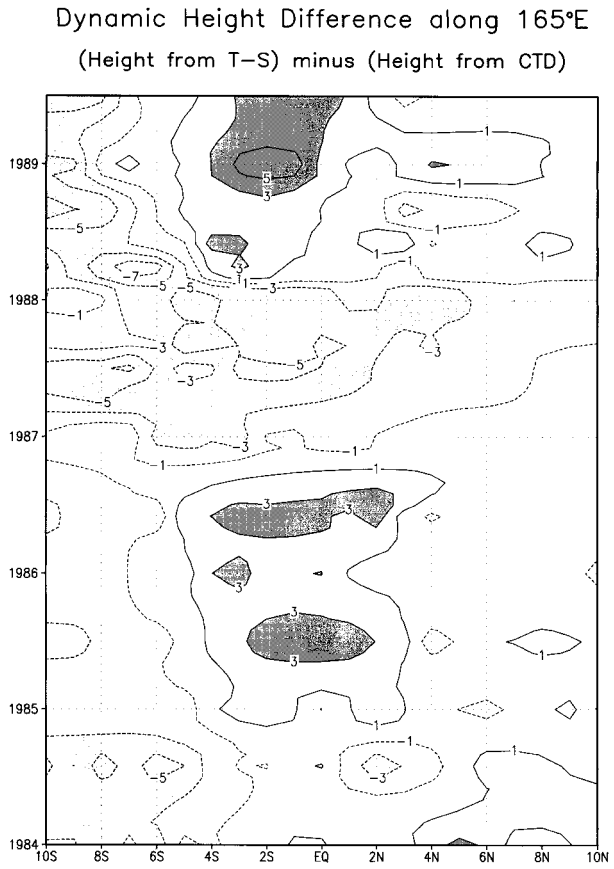

FIG. 10. The monthly dynamic height difference along 165°E on a 1° grid using CTD profile data. The contours are odd integers with shading above and below 3 dyn cm.

es in the thermocline made by the assimilation. It is through these changes to the model density structure and their subsequent effect on model dynamics that the assimilation of T/P data may impact ENSO prediction.

To further explore the patterns in the sea level difference that may impact ENSO prediction, we project the sea level error for the NCEP–XBT analyses, that is, NCEP–XBT minus NCEP–TP, onto empirical orthogonal functions (EOFs) of monthly mean sea level anomalies. The sea level EOFs were analyzed from a 16-yr (1980–95) monthly Pacific Ocean analysis dataset, which was produced from our ocean data assimilation system (Behringer et al. 1998). The spatial patterns of the first and second sea level EOFs are shown in the upper and middle panels of Fig. 11. The principal components of these two EOFs (not shown) indicate that the second EOF leads the first EOF by about a quarter period; they represent a ''cyclic'' behavior of ENSO. When the sea level error fields are projected onto the two leading EOFs, one can also compute the fraction of the total error variance accounted for by each of these two EOFs. These are also indicated in the figure.

The time evolution of the sea level error, when projected onto the first and second sea level EOFs, is shown in the lower panel of Fig. 11. We found that the sea level error has the largest projection on the second EOF. This EOF accounts for about 17.2% of the total sea level error variance with the largest amplitude found during 1996. All the other individual EOFs account for less than 5% of the total sea level error variance. The second EOF is regarded as the ''precursor'' of ENSO because it often has the largest amplitude during the onset (growing phase) of an ENSO event (e.g., Latif et al. 1990). Therefore a large error in the part of the anomalous sea level field described by the second EOF could lead to spurious evolution of the ENSO cycle.

If a significant amount of the sea level error projects onto the second sea level EOF, then the sea level error in the initial conditions could potentially impact the accuracy of the ENSO prediction. A systematic evaluation of that possibility will require a large number of ensemble predictions over a long time period. At present, we are unable to carry out those experiments. However, we have conducted a simple case study consisting of twin hindcasts for the winter of 1996/97. For one hindcast the ocean was initialized with an analysis that assimilated only temperature data, while for the other the ocean was initialized with a second analysis that assimilated T/P sea level data as well as temperature. The hindcasts were initiated in the summer of 1996 when the difference in sea level between these two analyses was large. The results of the case study (not shown) suggest that the inclusion the T/P sea level data in addition to subsurface temperature data in our present ocean data assimilation system could potentially have a positive impact on the accuracy of our ENSO prediction. The probable reason for this is that the assimilation of the T/P data alters the density structure and, hence, the dynamics of the ocean model. In the present assimilation system the upper ocean density field is changed only through changes to the temperature. However, there are times, as during the summer of 1996 when the hindcasts were initiated, when density changes in the upper ocean are actually caused by significant changes in salinity. The assimilation of T/P data into our present system can partially mitigate the system's inability to take into account the impact of salinity on density by relaxing the model fit to the temperature data while forcing an improved fit to sea level, resulting in a net improvement in upper ocean density.

7. Summary

In this paper, we have analyzed two sets of ocean analyses produced with data assimilation: one used only XBT and TAO data (NCEP–XBT), while the other used XBT and TAO plus T/P sea level data (NCEP–TP). A rising sea level trend is found in NCEP–XBT analysis in the western equatorial Pacific but this trend is essentially missing in NCEP–TP analysis. The trend results in sea level rise of 5–10 cm during 1995–96 period, which is a significant signal relevant to ENSO. We have

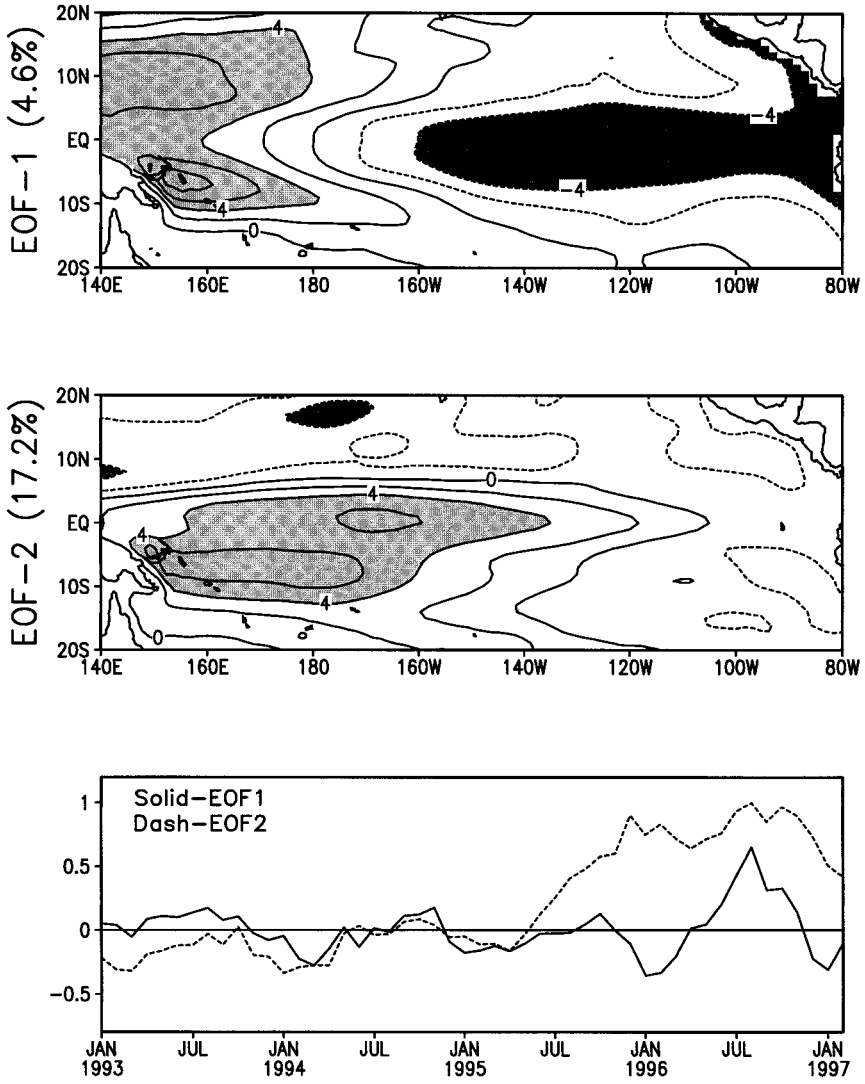

FIG. 11. Patterns of the two leading sea level anomaly EOFs [(a) and (b); contour interval is 2 dyn cm] and time evolution of the sea level errors (Jan 1993–Feb 1997) projected onto the two leading EOFs. The first and second EOFs account for 4.6% and 17.2% of the total sea level error variance, respectively.

also compared TAO-dynamic height and T/P sea level data and found a similar discrepancy in sea level trends in the western Pacific. However, the TAO-dynamic height computation used a mean *T*–*S* relationship because of lack of salinity observations. The similar discrepancy in sea level trends both in model–model comparisons and in direct–indirect observation comparisons strongly suggests to us that this is not a result of model—forcing field error, but the result of incomplete description of sea level variability by temperature observations alone.

One weakness of our present data assimilation system is that it is a univariate scheme. The assimilation of T/P data in our present system is done by correcting temperature field alone. Assimilation of altimetry data can result in positive changes in the salinity field toward reducing the sea level error through changes in the three-dimensional advection fields. However, large residual sea level errors remain because errors in the model and in the forcing fields prevent the model to have accurate salinity variations. The residual sea level errors must be compensated for by relaxing model–temperature data fit.

Our examinations of limited CTD observations provided further circumstantial evidence that the differing trends both in direct–indirect observation comparisons and in model–model comparisons could be caused by an underestimate of salinity variability. Our results indicate that a better method for ocean data assimilation would include corrections for both temperature and salinity, especially in the western Pacific. Salinity observations, especially subsurface salinity data, are very

sparse. A possible alternative is to use T/P sea level data to infer changes in subsurface salinity. We are currently approaching this problem using two different methods. The first approach (Vossepoel et al. 1999) assumes that the temperature observations are sufficient to correct the model temperature, and therefore any residual difference between the observed and model sea surface height can be used to correct the model salinity. The assumption is approximately valid in the equatorial Pacific within the domain covered by the TAO array. The second approach ties the variability in salinity and temperature together through a set of coupled empirical orthogonal modes based on historical data (Maes et al. 2000). Work is under way to improve our assimilation system by incorporating both of these methods into our T/P sea level data assimilation. The hope is that this will allow us to capture some of the large-scale interannual salinity variability using T/P data.

Another important question is whether the use of satellite altimetry data in addition to subsurface temperature data can improve the accuracy of ENSO prediction. Note that our attempt to explore the answer to this question is based on the current ocean observing network, which does not have the capability to observe subsurface salinity, and on the present ocean data assimilation technology. A systematic evaluation of the impact on ENSO prediction will require an estimate of the prediction skill and a test of the statistical significance of the skill based on a large number of ensemble hindcasts over a long period of time. This would require significant computational resources and a testing period that includes several ENSO episodes. The period when T/P data are available is not sufficiently long to carry out systematic hindcasting comparisons. However, our analyses show that the sea level error due to an underestimate of the salinity variability in the analysis system has a large projection on the second sea level EOF, which is often linked to the onset phase of ENSO events. This suggests that the sea level error may have a potential impact on the initialization of the ocean for ENSO prediction. We carried out a hindcasting case study and the results indicated that there may be occasions when the addition of T/P data can have positive impact on the ENSO prediction accuracy.

In the present assimilation system the density is changed only through changes to the temperature field. There is some risk in doing this if, as was true in our case study, some part of the modifications to temperature are done to compensate for errors in salinity. For example, if the temperature in the thermocline is changed to compensate for salinity errors in the surface layers, then the vertical structure of density will be distorted. It is therefore interesting to speculate that if our assimilation system were able to correct the density field by correcting salinity as well as temperature, the result might be further improvement in our ENSO prediction. Unfortunately, there are currently insufficient observations of salinity available to test this idea directly. However, a potentially practical solution would be a bivariate data assimilation system using sea level and temperature observations to correct both salinity and temperature. The goal of such a system would be to produce analyses that represent more accurate ocean initial conditions with consistent upper ocean temperature, salinity, and sea level variability.

Acknowledgments. Support for this research is provided by NOAA's Office of Global Program through the Climate and Global Change Program. Real-time TOPEX/Poseidon satellite altimetry data are provided by NOAA/Laboratory of Satellite Altimetry (R. Cheney). The CTD salinity data are kindly provided by Dr. Michael McPhaden of NOAA/PMEL. Dynamic heights from TAO moorings are kindly provided by Dr. W. Kessler of NOAA/PMEL. We thank M. McPhaden, W. Kessler (NOAA/PMEL), J. Picaut, C. Henin (ORSTOM), L. Miller (NOAA), F. Vossepoel (Delft University, Netherlands), A. Leetmaa (NOAA/NCEP), and three anonymous reviewers for their valuable comments and suggestions.

REFERENCES

Ando, K., and M. J. McPhaden, 1997: Variability of surface layer hydrography in the tropical Pacific Ocean. *J. Geophys. Res.*, **102,** 23 063–23 078.

Behringer, D. W., 1994: Sea surface height variations in the Atlantic Ocean: A comparison of TOPEX altimeter data with results from an ocean data assimilation system. *J. Geophys. Res.*, **99,** 24 685–24 690.

——, M. Ji, and A. Leetmaa, 1998: An improved coupled model for ENSO prediction and implications for ocean initialization. Part I: The ocean data assimilation system. *Mon. Wea. Rev.,* **126,** 1013–1021.

Bryan, K., 1969: A numerical method for the study of the World Ocean. *J. Comput. Phys.,* **4,** 347–376.

Busalacchi, A. J., M. J. McPhaden, and J. Picaut, 1994: Variability in equatorial Pacific sea surface topography during the verification phase of the TOPEX/Poseidon mission. *J. Geophys. Res.*, **99,** 24 725–24 738.

Carton, A. J., B. S. Giese, X.-H. Cao, and L. Miller, 1996: Impact of altimeter, thermistor, and XBT data on retrospective analyses of the tropical Pacific Ocean. *J. Geophys. Res.,* **101,** 14 147–14 159.

Chao, Y., and L. L. Fu, 1995: A comparison between the TOPEX/Poseidon data and global ocean general circulation model during 1992–1993. *J. Geophys. Res.*, **100,** 24 965–24 976.

Cheney, R., L. Miller, R. Agreen, N. Doyle, and J. Lillibridge, 1994: TOPEX/Poseodon: The 2-cm solution. *J. Geophys. Res.,* **99,** 24 555–24 564.

——, ——, J. Lillibridge, C.-K. Tai, and J. Kuhn, 1996: Near real-time altimetry from ERS-2 and TOPEX/Poseidon. *Eos, Trans. Amer. Geophys. Union,* **77** (46), F129.

Cox, M. D., 1984: A primitive, 3-dimensional model of the ocean. GFDL Ocean Group Tech. Rep. 1, 143 pp. [Available from NOAA/Geophysical Fluid Dynamics Laboratory, Princeton University, Princeton, NJ 08540.]

Cressman, G. P., 1959: An operational objective analysis system. *Mon. Wea. Rev.,* **87,** 367–374.

Derber, J. D., and A. Rosati, 1989: A global oceanic data assimilation system. *J. Phys. Oceanogr.,* **19,** 1333–1347.

Emery, W. J., and J. S. Dewar, 1982: Mean temperature-salinity, salinity-depth and temperature-depth curves for the North At-

lantic and North Pacific. *Progress in Oceanography,* Vol. 11, Pergamon, 219–305.
Fischer, M., M. Latif, M. Flugel, and M. Ji, 1997: On the benefit of sea level assimilation in the tropical Pacific. *Mon. Wea. Rev.*, **125,** 819–829.
Ji, M., and A. Leetmaa, 1997: Impact of data assimilation on ocean initialization and El Nino prediction. *Mon. Wea. Rev.,* **125,** 742–753.
——, ——, and J. Derber, 1995: An ocean analysis system for seasonal to interannual climate studies. *Mon. Wea. Rev.,* **123,** 460–481.
Kessler, W. S., 1999: Interannual variability of the subsurface high salinity tongue south of the equator at 165°E. *J. Phys. Oceanogr.,* **29,** 2038–2049.
——, and B. A. Taft, 1987: Dynamic heights and zonal geostrophic transports in the central tropical Pacific during 1974–84. *J. Phys. Oceanogr.,* **17,** 97–122.
Latif, M., J. Biercamp, H. von Storch, M. J. McPhaden, and E. Kirk, 1990: Simulation of ENSO related surface wind anomalies with an atmospheric GCM forced by observed SST. *J. Climate,* **3,** 509–521.
Levitus, S., R. Burgett, and T. P. Boyer, 1994: *Salinity.* Vol. 3, *World Ocean Atlas 1994,* NOAA Atlas NESDIS 3, U.S. Dept. of Commerce, 99 pp.
Maes, C., 1998: Estimating the influence of salinity on sea level anomaly in the ocean. *Geophys. Res. Lett.,* **25,** 3551–3554.
——, D. W. Behringer, R. W. Reynolds, and M. Ji, 2000: Retrospective analysis of the salinity variability in the western tropical Pacific Ocean using an indirect minimization approach. *J. Atmos. Oceanic. Technol.,* in press.
McPhaden, M. J., 1993: TOGA-TAO and the 1991–93 El Niño–Southern Oscillation event. *Oceanography,* **6** (2), 36–44.
——, S. P. Hayes, L. J. Mangum, and J. M. Toole, 1990: Variability in the western equatorial Pacific Ocean during the 1986–87 El Niño/Southern Oscillation event. *J. Phys. Oceanogr.,* **20,** 190–208.
——, and Coauthors, 1998: The Tropical Ocean Global Atmosphere (TOGA) observing system: A decade of progress. *J. Geophys. Res.,* **103** (C7), 14 169–14 240.
Oberhuber, J. M., 1988: An atlas based on the ''COAS'' data set: The budgets of heat, buoyancy and turbulent kinetic energy at the surface of the global ocean. Rep. 15, 20 pp. [Available from Max-Planck Institut für Meteorologie, Bundesstrasse 55, Hamburg, Germany.]
Philander, S. G. H., W. J. Hurlin, and A. D. Seigel, 1987: A model of the seasonal cycle in the tropical Pacific Ocean. *J. Phys. Oceanogr.,* **17,** 1986–2002.
Picaut, J., A. J. Busalacchi, M. J. McPhaden, L. Gourdeau, F. I. Gonzalez, and E. C. Hackert, 1995: Open-ocean validation of TOPEX/Poseidon sea level in the western equatorial Pacific. *J. Geophys. Res.,* **100,** 25 109–25 127.
Pinardi, N., A. Rosati, and R. C. Pacanowski, 1995: The sea surface pressure formulation of rigid lid models. Implications for altimetric data assimilation studies. *J. Mar. Syst.,* **6,** 109–119.
Vossepoel, F. C., R. W. Reynolds, and L. Miller, 1999: Use of sea level observations to estimate salinity variability in the tropical Pacific. *J. Atmos. Oceanic Technol.,* **16,** 1401–1415.
Wyrtki, K., 1979: Sea level variations: Monitoring the breath of the Pacific. *Eos, Trans. Amer. Geophys. Union,* **60,** 25–27.